

Modeling of 2-DOF Hexapod Leg Using Analytical Method

Agusma Wajiansyah¹, Supriadi^{2*}, Achmad Fanany Onnilita Gaffar³, Arief Bramanto Wicaksono Putra⁴
^{1,2,3,4} Department of Information Technology, Politeknik Negeri Samarinda, East Kalimantan, Indonesia
Email: ¹ agusma.wajiansyah@gmail.com, ² supriadi.polnes@gmail.com,
³ onnygaffar212@gmail.com, ⁴ ariefbram@gmail.com
*Corresponding Author

Abstract— Walking robot is one type of mobile platform that has locomotion type "walking." DOF (Degree of Freedom) is one of essential character for the design of robot mechanism based on its models. Legs are the critical parts of the walking robot structure. The legged robot is the walking robot biologically adopted from animal or insect behavior, especially in their walking routine. The hexapod robot is one of the most statically stable legged robots and has high flexibility when standing or moving which supported by six legs that can be easily manipulated. For modeling needs and its validation, it is desirable to control each DOF in the space of Cartesian coordinate although motor system needs the reference inputs in the joint space. In this case, it needs to know the conversion between Cartesian and joint space, inverse, and forward kinematics. This study presents a kinematic model of the 2-DOF hexapod leg. This study aimed to build a kinematic model of the 2-DOF hexapod leg using an analytical approach. Analytically, the working mechanism of the robot can be modeled using forward and inverse kinematic models. In this method, this modeling is derived mathematically from the projection analysis of the movement in a certain coordinate space. The model validation was performed using the MATLAB tool and the Robotic Toolbox. The results of this study showed that the results of the inverse kinematic process have the same output signal pattern compare to the input signal pattern of the forward kinematic process.

Keywords— Degree of Freedom, 2-DOF hexapod leg, kinematic model analytical approach

I. INTRODUCTION

Mobile Manipulator (MM) is a concept to extend the workspace of robot manipulators that can be deported on mobile platforms. The use of mobile platforms overcomes the problem of limited workspace. Mobile platforms classified by their type of locomotion (crawling, walking or rolling), their speed or their maximal payload. Mobile robots are sorted by numerous criteria. [1]. The first classification of mobile robots considers the environment in which they are supposed to evolve such as aerial [2-9], terrestrial [10-14], marine [15-17] or submarine [18-23].

Walking robot is one type of mobile platform that has locomotion type "walking." Legs are the critical parts of the walking robot structure. The legged robot can explore rugged terrain with obstacles and rocks that are hard to do with the wheeled robot. Design of robot mechanism based on the types of mechanisms primarily determined several basic characters such as the degree of freedom (DOF), workspace, etc. A specific type synthesis method for designing of walking robot

legs is one of the powerful tools for improving the operating performance [24]. The legged robot is biologically inspired by animal or insect behavior, especially in their walking behavior. A hexapod robot is a robot that moves to utilize six legs. Statistically, robots remain stable by using 3 legs or more; hence, a hexapod robot has high stability and flexibility. In the case of the faulty leg, the possibility of the robot to move remains [25]. A gait defined as the locomotion through the movement of robot legs. The legged chassis commonly has more than two legs, so the locomotion of a robot is much more complicated. There are several basic gaits, such as a tripod, wave or ripple. A wave/ripple gait used for a slowly walking while a tripod gait used for a faster walking [26].

Each gait of hexapod has a sequence of joint angle steps that make the hexapod move from one position to another. This setting can be done with a lookup table method that is computationally easier. However, this method does not provide flexibility in moving. In this case, every position shift must be controlled starts with controlling each hexapod footrest position. One approach is to use a mathematical formulation or reversed kinematics model by ignoring other mechanical friction factors or losses [27]. Kinematic modeling of hexapod has the widely researched robotic machining challenges which translated to achievable tolerance ranges in real-world production for the general purpose of applications [28]. For modeling needs and its validation, it is desirable to control each DOF in the space of Cartesian coordinate although motor system needs the reference inputs in the joint space. In this case, it needs to know the conversion between Cartesian and joint space, inverse, and forward kinematics. Forward kinematics gives the position of hexapod for the given joint angles. Inverse kinematics is employed to reach the desired position of the hexapod [29]. There are much research has been done about kinematic models of robotic systems for various purposes [20, 29-34].

This study presents a kinematic model of the 2-DOF hexapod leg. This study aimed to build a kinematic model of the 2-DOF hexapod leg using an analytical approach. Model validation has done using the MATLAB tool and Robotic Toolbox.



II. MATERIALS AND METHOD

In the context of the design of a robot, the analytical approach is a fact-based method to understand how the working mechanism of a robot behaves in a particular workspace. Analytically, the working mechanism of a robot can be modeled using a forward and inverse kinematic model. This modeling is derived mathematically from movement projection analysis within a particular coordinate space. Forward and inverse kinematics is the necessary method for the hexapod leg mechanism to determine where for hexapod robot starts from each leg. The forward kinematic finds geometric parameters from the tip of the leg (position on Cartesian coordinate space X, Y, Z) based on the rotation angle of the joints of each leg. The inverse kinematic finds the rotation angle of the joints of each leg based on the given geometry parameters.

Because hexapod is in a particular workspace, in principle the motion mechanism of each leg can be viewed separately. Furthermore, the integration of all kinematic models of each leg can be used to build a complete hexapod kinematic model. This section presents the kinematic modeling of 2 DOF hexapod legs by using an analytical approach

A. 2-DOF Hexapod Leg

Workspace planning is essential for the design of a legged robot especially concerning the adoption of selected animal or insect behavior. Generally, the hexapod design uses workspaces in the form of Cartesian or Radial coordinate systems or transformations between them. The hexapod robot is a robotic system that consists of a rigid body and six legs with 2-DOF while each leg has the same structure. Each DOF is represented by a joint that is commonly driven by a servo motor, and other types of drivers and actuators depend on the design objectives. The physical model of the hexapod robot shown in Fig. 1. Commonly, the body structure and hexapod legs positions are designed in such a way by referring to the division of quadrants from a full circle angle. In this way, the kinematic modeling of each leg can be done separately. It aims for ease in making of kinematic models.

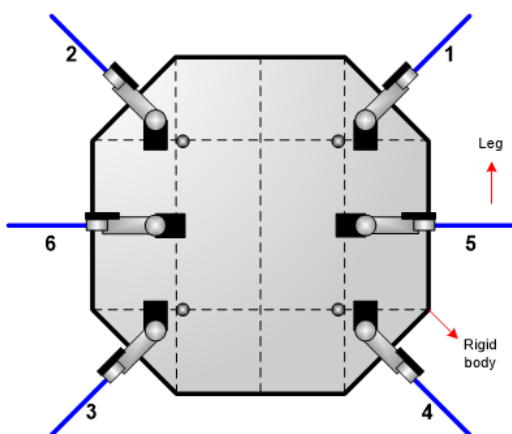


Fig. 1. The hexapod robot (top view)

If the tip of each hip leg is at the origin of the Cartesian coordinates, then it can be described as shown in Fig. 2. Positions of leg 1 to 4 are in quadrant 1, quadrant 2, quadrant 3, and quadrant 4, respectively. Especially for the positions of leg 5 and six are between quadrants 4 and 1 and quadrants

2 and 3, respectively. In principle, each leg is in the same workspace shape, only different reference to its original point if combined. For this reason, the kinematic analysis of each hexapod leg displacement can be performed on the same workspace in Cartesian coordinates.

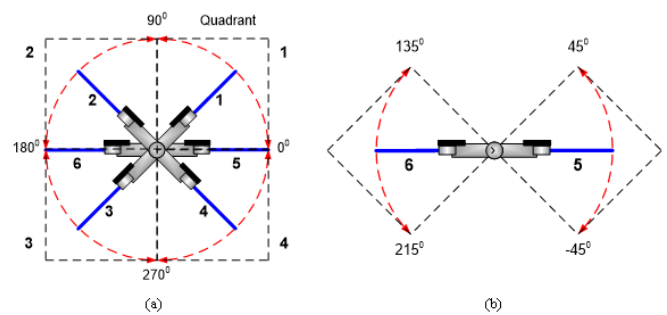


Fig. 2. Workspace of all hexapod legs in Cartesian coordinate

In this study, the kinematic analysis was performed using quadrant 1. Each leg consists of the coxa and tibia parts. Each of these parts has joints. Their joint rotation represents their displacement. For each displacement of the joint rotation was described by using a different Cartesian coordinate plane. The angle rotation of the tibia part presented in the XZ plane while the angular rotation of the coxa part displayed in the XY plane. The physical model of 2-DOF hexapod leg shown in Fig. 3. The joint rotation of the coxa part denoted by z_0 and joint rotation of the tibia part denoted by z_1 .

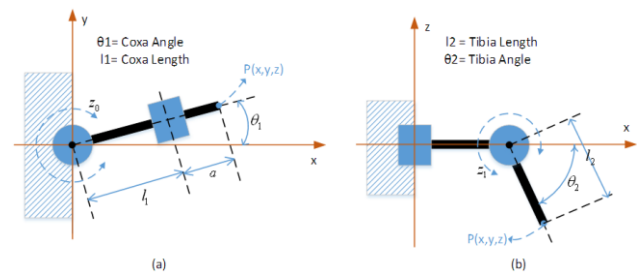


Fig. 3. Physical model of the hexapod leg: (a). top view (XY plane); (b). side view (XZ plane)

The position of the tip of the leg denoted by $P(x, y, z)$. The position of point P against the XYZ plane determined by the angle θ_1 and θ_2 mathematically expressed by:

$$P(x, y, z) = f(\theta_1, \theta_2) \tag{1}$$

where θ_1 is the coxa angle and θ_2 is the tibial angle

B. Kinematic Analysis

Referring to Fig. 3, the coordinate system of the leg joints can be illustrated by the vector form as shown in Fig. 4. Point P can also be obtained by summing the vectors formed by the coxa and tibia parts, which can be expressed by:

$$P(x, y, z) = \vec{l}_1 + \vec{l}_2 \tag{2}$$

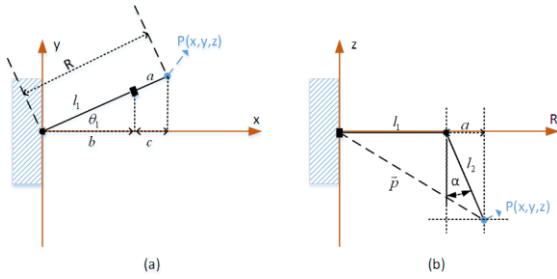


Fig. 4. The coordinate system of the leg joints: (a). XY plane; (b). XZ plane

In the XY plane, R is the vector connecting the point P with the origin. R is the sum of the vectors of \vec{l}_1 and a where a is the projection result of \vec{l}_2 toward R. In this case, \vec{l}_1 and \vec{l}_2 can be stated by:

$$\vec{l}_1(x_1, y_1, z_1) \begin{cases} x_1 = l_1 \cos \theta_1 \\ y_1 = l_1 \sin \theta_1 \\ z_1 = 0 \end{cases} \quad (3)$$

$$\vec{l}_2(x_2, y_2, z_2) \begin{cases} x_2 = a \cdot \cos \theta_1 \\ y_2 = l_2 \cdot \sin \theta_1 \\ z_2 = l_2 \cdot \sin \alpha \end{cases} \quad (4)$$

Assuming that θ_2 has a movement of 90° , then:

$$\alpha = 90 - \theta_2 \quad a = l_2 \cdot \sin \alpha \quad (5)$$

By substitutions (3) and (4) to (2) then obtained:

$$P(x, y, z) = (x_1, y_1, z_1) + (x_2, y_2, z_2) \quad (6)$$

$$= (x_1 + x_2, y_1 + y_2, z_1 + z_2)$$

Where

$$\begin{aligned} x &= l_1 \cos \theta_1 + a \cdot \cos \theta_1 \\ &= l_1 \cos \theta_1 + l_2 \cdot \sin(90 - \theta_2) \cdot \cos \theta_1 \\ y &= l_1 \sin \theta_1 + a \cdot \sin \theta_1 \\ &= l_1 \sin \theta_1 + l_2 \cdot \sin(90 - \theta_2) \cdot \sin \theta_1 \\ z &= l_2 \cdot \cos(90 - \theta_2) \end{aligned} \quad (7)$$

In the matrix form stated by:

$$\begin{bmatrix} x \\ y \\ z \end{bmatrix} = \begin{bmatrix} \cos \theta_1 & \sin(90 - \theta_2) \cdot \cos \theta_1 & 0 \\ \sin \theta_1 & \sin(90 - \theta_2) \cdot \sin \theta_1 & 0 \\ 0 & \cos(90 - \theta_2) & 0 \end{bmatrix} \begin{bmatrix} l_1 \\ l_2 \\ 0 \end{bmatrix} \quad (8)$$

Equation (8) is used to determine the position in the Cartesian coordinate based on its angular rotation (Forward Kinematic). Inverse kinematics is employed to reach the desired position of the hexapod leg. In this case, the angle value of the joint based on the desired position expressed by:

$$\theta_1 = \tan^{-1} \left(\frac{y}{x} \right) \quad (9)$$

Referring to Fig. 4 (b), as a result of angular movement θ_2 , there will be $\vec{l}_1 \vec{l}_2 p$ triangle as shown in Fig. 5. By using trigonometric rules, the magnitude of vector p expressed by:

$$|p|^2 = l_1^2 + l_2^2 - 2l_1 l_2 \cdot \cos \beta \quad (10)$$

Where β obtained by using the following formula:

$$\beta = \cos^{-1} \frac{l_1^2 + l_2^2 - |p|^2}{2l_1 l_2} \quad |p|^2 = x^2 + y^2 + z^2 \quad (11)$$

Thus, variable θ_2 can be stated by:

$$\theta_2 = 180 - \beta \quad (12)$$

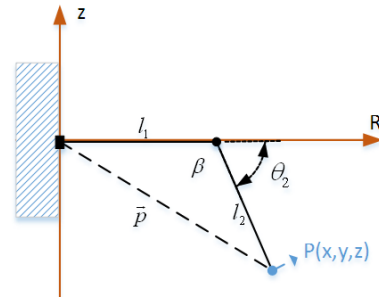


Fig. 5. The $\vec{l}_1 \vec{l}_2 p$ triangle

III. RESULTS AND DISCUSSION

Testing of the kinematic model of the 2-DOF hexapod leg has been made perform by using MATLAB programming and Robotic Toolbox tools. Suppose $\theta_1=0, \theta_2 = 30^\circ, l_1=10, l_2=5$, then by using (8) obtained $P_1(x, y, z) = (14.3301, 0, -2.5)$ as shown in Fig. 6. If θ_1 is rotated for 20° , then the position of the tip of leg moves to $P_2(x, y, z) = (13.4659, 4.9012, -2.5)$ as shown in Fig. 7.

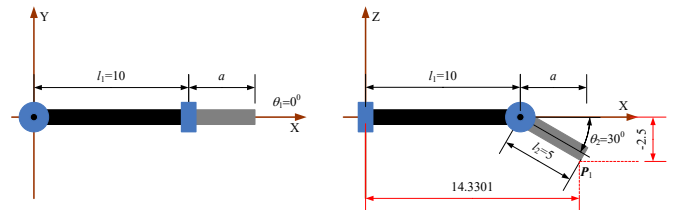


Fig. 6. The position of the tip of leg (P1) by $\theta_1=0, \theta_2 = -30^\circ, l_1=10, l_2=5$

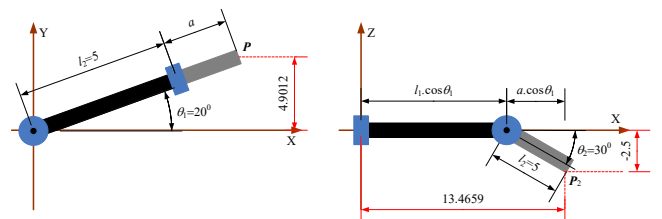


Fig. 7. The position of the tip of leg (P2) by $\theta_1 = 20^\circ, \theta_2 = -30^\circ, l_1 = 10, l_2 = 5$

For the inverse kinematic model, the two positions (P_1 and P_2) used as input parameters to obtained θ_1 and θ_2 by using (9) – (12). By the same parameters, the test results using Robotic Toolbox was shown in Fig. 8 and Fig. 9

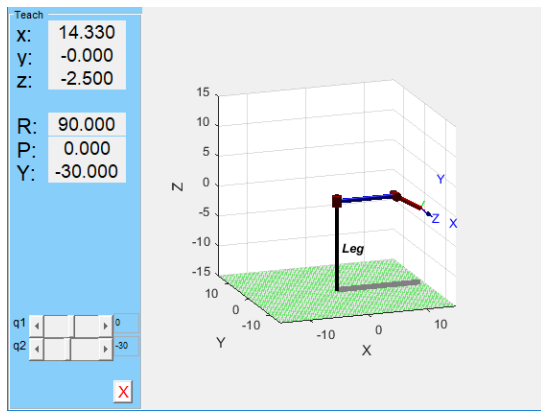


Fig. 8. The testing results using Robotic toolbox with $\theta_1 = 0, \theta_2 = -30^\circ, l_1 = 10, l_2 = 5$

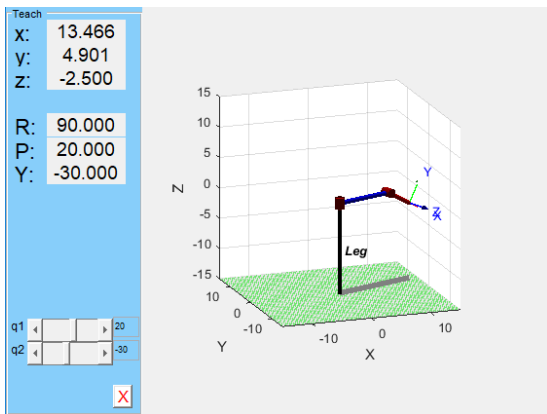


Fig. 9. The testing results using Robotic toolbox with $\theta_1 = 20^\circ, \theta_2 = -30^\circ, l_1 = 10, l_2 = 5$

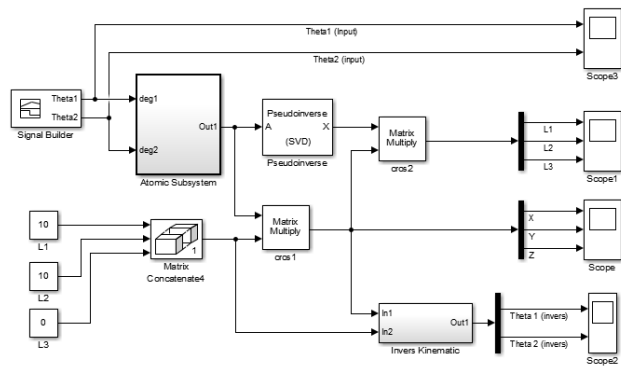


Fig. 10. The Simulink model for test the built kinematic model

Testing was also done by using Simulink MATLAB to know the response of the built kinematic model by variation of angle rotation. The model used as shown in Fig. 9. The input signal in the form of angular change is generated by using the Signal Builder where θ_1 within the range $\{0^\circ \dots 20^\circ\}$ and θ_2 within the range $\{-90^\circ \dots -50^\circ\}$. The movement planning was shown in Table 1 while their input signal patterns were shown in Fig. 11.

TABLE I. MOVEMENT PLANNING

No	Time sequence (t)	description	θ_1	θ_2
1	0	Start point	0°	-90°
2	0 - 2	No movement	0°	-90°
3	2 - 7	coxa part no movement tibia part move as far as 40°	0°	-50°
4	7 - 11	coxa part move as far as 20° tibia part no movement	20°	-50°
5	11 - 15	coxa part no movement tibia part no movement	20°	-50°
6	15 - 20	coxa part move as far as -20° tibia part move as far as -40°	0°	-90°
7	20 >	idle		

From Fig. 11 indicates that the input signal was given alternately up to $t = 11$ sec. At time $t = 11 - 15$ sec there was no change of input signal, whereas between $t = 15 - 20$ sec given the input signal simultaneously. These input signal patterns were used to perform the forward kinematic process. The results of this process were shown in Fig. 11. The result showed that the angular change of θ_2 within $t = 2 - 7$ sec only affects the displacement of its position in the XZ plane while the angular change of θ_1 within $t = 7 - 11$ sec only affects the displacement of its position in the XY plane. For the given θ_1 and θ_2 signals simultaneously affect the displacement of its position simultaneously both in the XY plane and in the XZ plane. From the results of this forward kinematic model has proved that the input signal pattern planning was very determining the mechanism of the desired hexapod leg movements.

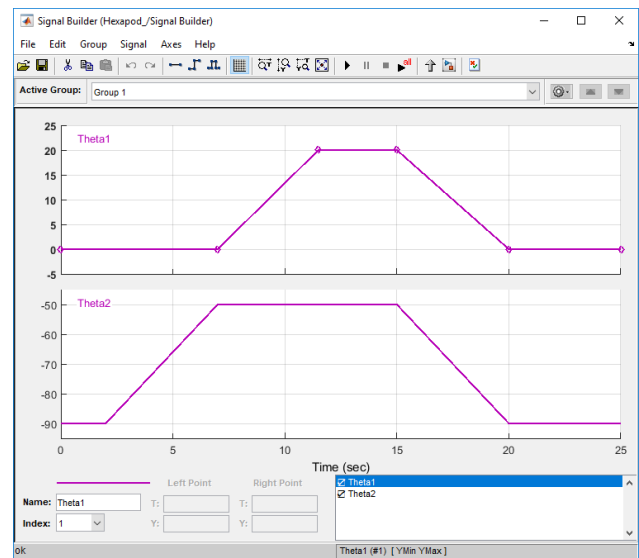


Fig. 11. The planned input signal pattern of the forward kinematic process

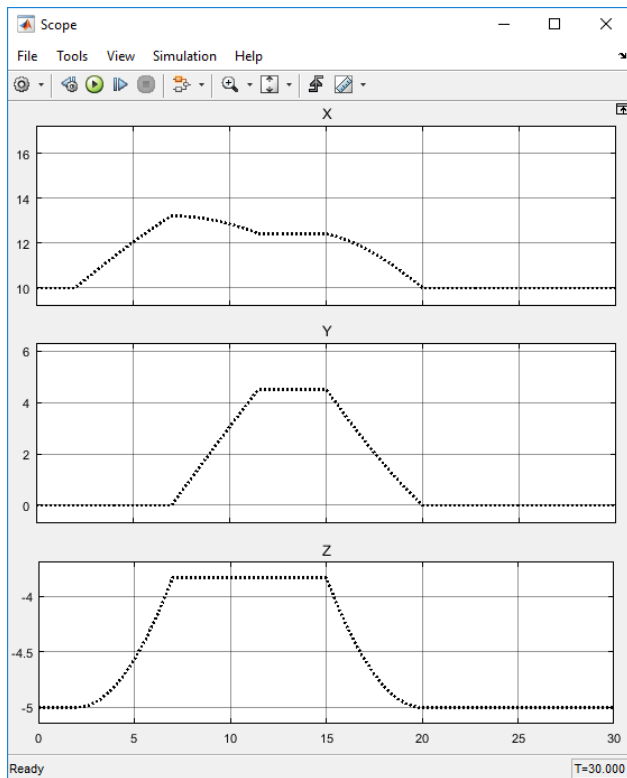


Fig. 12. The position changes of tip of leg

Each position of the tip of leg as shown in Fig. 12 was then used to perform the inverse kinematic process. The results of this process were shown in Fig. 13. The output signal generated from the inverse kinematic process as shown in Fig. 12 has the same pattern as the input signal generated using the signal builder as shown in Fig. 11. This indicates that the mathematical model that has been made has successfully represented the kinematic process of the hexapod leg. Visually, the result of kinematic inverse process was shown in Fig. 14

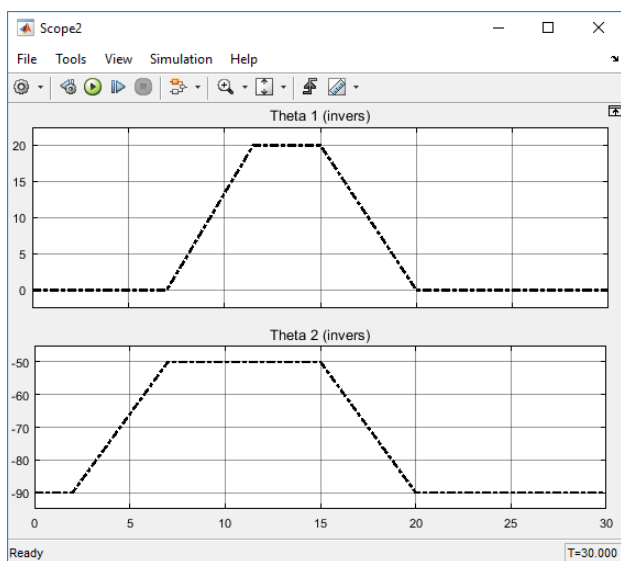


Fig. 13. The results of the inverse kinematic process

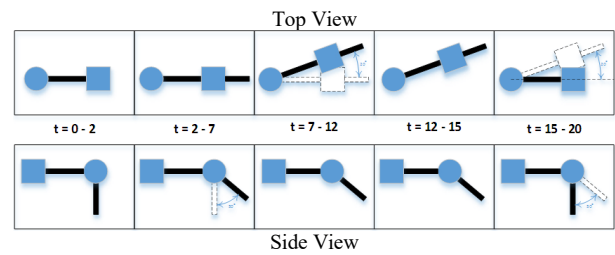


Fig. 14. Visualization of the results of the inverse kinematic process

IV. CONCLUSION

Because the hexapod design uses workspaces in the form of Cartesian coordinate, in principle the motion mechanism of each leg can be viewed separately based on the quadrant position of each leg. In this study, the kinematic analysis was performed using quadrant 1. The kinematic model of 2 DOF hexapod legs has presented in this study with an analytic approach. The results of this study showed that the results of the inverse kinematic process have the same output signal pattern compare to the input signal pattern of the forward kinematic process. In fact, a kinematic inverse model is used to obtain the *coxa* and *tibia* angles of the hexapod leg to move on the desired position. The *coxa* and *tibia* angle will be used as input signal for driver or actuator of each joint.

For further study, the all kinematic model of each hexapod leg needs to be integrated into the same workspace to obtain a complete hexapod kinematic model.

REFERENCES

- [1] Rubio F, Valero F, Llopis-Albert C. "A review of mobile robots: Concepts, methods, theoretical framework, and applications", *International Journal of Advanced Robotic Systems*. March 2019.
- [2] S. Basu, A. Omotubora, M. Beeson, and C. Fox, "Legal framework for small autonomous agricultural robots," *Ai & Society*, 2018.
- [3] E. Vlasceanu, D. Popescu and L. Ichim, "Aerial Robotic Team for Complex Monitoring in Precision Agriculture," *15th International Conference on Distributed Computing in Sensor Systems (DCOSS)*, Santorini Island, Greece, 2019.
- [4] J. Dentler, S. Kannan, S. Bezzaoucha, M. A. Olivares-Mendez, and H. Voos, "Model predictive cooperative localization control of multiple UAVs using potential function sensor constraints," *Autonomous Robots*, 2018.
- [5] M. L. Ireland and D. Anderson, "Optimisation of Trajectories for Wireless Power Transmission to a Quadrotor Aerial Robot," *Journal of Intelligent & Robotic Systems*, 2018.
- [6] C. Sampedro et al., "A fully-autonomous aerial robotic solution for the 2016 International Micro Air Vehicle competition," *International Conference on Unmanned Aircraft Systems (ICUAS)*, Miami, FL, USA, 2017.
- [7] A. Rodriguez-Ramos, C. Sampedro, H. Bavle, Z. Milosevic, A. Garcia-Vaquero and P. Campoy, "Towards fully autonomous landing on moving platforms for rotary Unmanned Aerial Vehicles," *International Conference on Unmanned Aircraft Systems (ICUAS)*, Miami, FL, USA, 2017.
- [8] A. U. Shamsudin, K. Ohno, R. Hamada, S. Kojima, T. Westfechtel, T. Suzuki, Y. Okada, S. Tadokoro, J. Fujita, and H. Amano, "Consistent map building in petrochemical complexes for firefighter robots using SLAM based on GPS and LIDAR," *ROBOMECH Journal*, vol. 5, 2018.
- [9] H.-S. Shin, A. F. Antoniadis, and A. Tsourdos, "Parametric Study on Formation Flying Effectiveness for a Blended-Wing UAV," *Journal of Intelligent & Robotic Systems*, 2018.
- [10] M. M. Ali, A. A. Abdulla, N. Stoll, and K. Thurow, "Mobile Robot Transportation for Multiple Labware with Hybrid Pose Correction in Life Science Laboratories," *Journal of Automation, Mobile Robotics & Intelligent Systems*, vol. 11, 2018.
- [11] A. Latif, K. Shankar, P. Thanh Nguyen, "Legged Fire Fighter Robot Movement Using PID" *Journal of Robotic and Control*, Vol 1, Issue 1, 2020.

- [12] A. Latif, A. Widodo, R. Rahim, K. Kunal, "Implementation of Line Follower Robot based Microcontroller ATmega32A", *Journal of Robotics and Control*, Vol 1, No 2, March 2020.
- [13] A. M. Martins, P. J. Alsina and R. C. Pereira, "Planar target following control scheme based on path generation for nonholonomic terrestrial robots," *Latin American Robotics Symposium (LARS) and Brazilian Symposium on Robotics (SBR)*, Curitiba, 2017.
- [14] S. Sendari, M. S. Hadi, A. N. Handayani, Y. R. Wahyudi and H. Lin, "Implementation of PD (Proportional Derivative) Control System On Six-Legged Wall Follower Robot," *International Automatic Control Conference (CACCS)*, Taoyuan, 2018.
- [15] L. V. Kiselev, A. V. Medvedev, V. B. Kostousov and A. E. Tarkhanov, "Autonomous underwater robot as an ideal platform for marine gravity surveys," *24th Saint Petersburg International Conference on Integrated Navigation Systems (ICINS)*, St. Petersburg, 2017.
- [16] M. Kim, G. R. Cho, H. Kang, S. C. Jee and J. Li, "Prototype development of underwater vehicle overcoming strong current," *14th International Conference on Ubiquitous Robots and Ambient Intelligence (URAI)*, Jeju, 2017.
- [17] J. Wampler, B. Li, T. Mosciki, and K. D. v. Ellenrieder, "Towards Adjustable Autonomy for Human-Robot Interaction in Marine Systems," *IEEE Transaction*, 2017.
- [18] S. Chauré, P. Chavan, S. Dhavale, and V. B. Jagtap, "Underwater Metal Detecting Robot using Wireless Communication," *International Journal Of Innovations In Engineering Research And Technology [Ijiert]*, vol. 4, pp. 16-21, 2017.
- [19] J. A. M. Anieva, T. S. Jimenez, L. G. G. Valdovinos, L. N. Balanzar and J. P. O. Muniz, "Design, Modeling and Control of a Micro AUV," *OCEANS 2018 MTS/IEEE Charleston*, Charleston, SC, pp. 1-7, 2018
- [20] M. Dong, W. Chou, and B. Fang, "Vertical Motion Control of Underwater Robot Based on Hydrodynamics and Kinematics Analysis," *IEEE Transaction*, 2017.
- [21] L. Furno, M. Blanke, R. Galeazzi, and D. J. Christensen, "Self-reconfiguration of modular underwater robots using an energy heuristic," *IEEE/RSJ International Conference on Intelligent Robots and Systems (IROS)*, Vancouver, BC, Canada, 2017.
- [22] R. Sundar, M. Dheepak, and P. V. Kumar, "PC Based Remote Operated Underwater Vehicle for Marine Surveillance," *International Journal of Civil Engineering and Technology (IJCIET)*, vol. 8, pp. 716-721, 2017.
- [23] A. C. Viñas, "Robot Learning applied to Autonomous Underwater Vehicles for intervention tasks," Doctoral Program, Doctoral Program in Technology, University of Girona, Girona, 2017.
- [24] D. Xi and F. Gao, "Type Synthesis of Walking Robot Legs," *Chinese Journal of Mechanical Engineering*, vol. 31, 2018.
- [25] Q. Hidayati, F. Z. Rachman, N. Yanti, "Intelligent Control System of Fire-Extinguishing and Obstacle-Avoiding Hexapod Robot," *Kinetik. Vol 3, No 1*, 2018
- [26] R. Pavan, T. Robin, C. Raphael, A. Thibault, B. Richard, A. Jan, Ijspeert, A.J, F. Dario, "Climbing favours the tripod gait over alternative faster insect gaits." *Nature Communications*, 2017.
- [27] A. Papacharalampopoulos, P. Aivaliotis, and S. Makris, "Simulating robotic manipulation of cabling and interaction with surroundings," *The International Journal of Advanced Manufacturing Technology*, vol. 96, pp. 2183-2193, 2018.
- [28] J. D. Barnfather, M. J. Goodfellow, and T. Abram, "Achievable tolerances in robotic feature machining operations using a low-cost hexapod," *The International Journal of Advanced Manufacturing Technology*, vol. 95, pp. 1421-1436, 2017.
- [29] A. Patil, M. Kulkarni, and A. Aswale, "Analysis of the inverse kinematics for 5 DOF robot arm using D-H parameters," in *Conference on Real-time Computing and Robotics*, Okinawa, Japan, 2017.
- [30] E. Bjoerlykhaug, "A Closed Loop Inverse Kinematics Solver Intended for Offline Calculation Optimized with GA," *Robotics*, vol. 7, p. 7, 2018.
- [31] J. Sun, G. Cao, W. Li, Y. Liang and S. Huang, "Analytical inverse kinematic solution using the D-H method for a 6-DOF robot," *14th International Conference on Ubiquitous Robots and Ambient Intelligence (URAI)*, Jeju, 2017.
- [32] S. S. R. CH, S. Patlolla, A. Agrawal, and A. K. R., "HexaMob—A Hybrid Modular Robotic Design for Implementing Biomimetic Structures," *Robotics*, vol. 6, p. 27, 2017.
- [33] G. R. U, D. A. A, P. S. S, E. S. B, and S. V. B, "Kinematics Analysis of Various Robot Configurations," *International Research Journal of Engineering and Technology (IRJET)* vol. 4, pp. 921-933, 2017.
- [34] S. Fuenzalida, K. Toapanta, J. Paillacho and D. Paillacho, "Forward and Inverse Kinematics of a Humanoid Robot Head for Social Human Robot-Interaction," *IEEE Fourth Ecuador Technical Chapters Meeting (ETCM)*, Guayaquil, Ecuador, 2019.